Chemically Modified Electrodes. 10. Electron Spectroscopy for Chemical Analysis and Alternating Current Voltammetry of Glassy Carbon-Bound Tetra(aminophenyl)porphyrins

John C. Lennox and Royce W. Murray*[1]

Contribution from the Kenan Laboratories of Chemistry, University of North Carolina, Chapel Hill, North Carolina 27514. *Received November 17, 1977*

Abstract: ESCA data show that tetra(aminophenyl)porphyrin is bound to glassy carbon electrode surfaces by an average of two amide bonds. The bound porphyrin, its Co-metalated analogue, and a nitroaromatic bound to the porphyrin via the dangling amine sites exhibit electrochemical surface waves detected by cyclic, differential pulse and ac voltammetry. Axial coordination of immobilized porphyrin is demonstrated by sensitivity of the electrochemistry to added bases.

We recently applied the carbon amidization reaction sequence (eq 1) described for chiral electrodes by Watkins et al.[2]

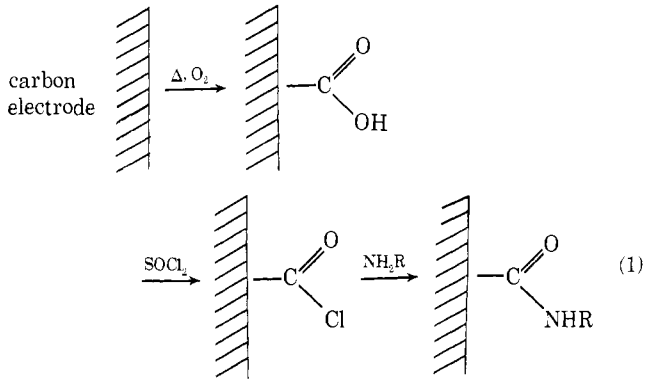

(1)

to the covalent binding of tetra(aminophenyl)porphyrin to glassy carbon electrode surfaces.[3] The thus immobilized porphyrin, designated C-T(NH_2)PP, is electrochemically reactive, exhibiting reversible cyclic voltammetric waves in solutions devoid of dissolved porphyrin, at potentials close to those of cyclic voltammograms of dissolved T(NH_2)PP in conventional solutions. C-T(NH_2)PP electrode surfaces can furthermore be metalated with Co(II), after which electrochemical reduction of CoT(NH_2)PP is observed. Electrochemical and ESCA control experiments demonstrated[3] that the observed porphyrin immobilization, under the circumstances of our experiments, depends on amide bonding as in reaction 1, as distinct from adsorption of porphyrin from aqueous solutions onto carbon reported by Anson et al.[4,5]

Results of further experiments on glassy carbon-immobilized T(NH_2)PP and CoT(NH_2)PP are presented in this paper. The number of amide bonds formed between the tetra(aminophenyl)porphyrin and the carbon surface has been determined by ESCA derivatization analysis, and electrochemical effects of axial coordination of immobilized CoT(NH_2)PP are observed. The excellent sensitivity of phase-selective ac voltammetry for surface redox processes proved important in experiments on surfaces bearing both T(NH_2)PP and CoT(NH_2)PP.

Experimental Section

Preparation and binding of tetra(*m*-aminophenyl)porphyrin, T(*m*-NH_2)PP, and tetra(*p*-aminophenyl)porphyrin, T(*p*-NH_2)PP, to glassy carbon was performed as detailed previously. Metalation was by warming with $CoCl_2$ in DMF or CH_3CN. The para and ortho isomers of monoaminotetraphenylporphyrin, M(NH_2)TPP, were generous gifts from C. M. Elliott (Stanford University). For investigation of amide binding, electrodes to which T(*m*-NH_2)PP had been bound were reacted with 3,5-dinitrobenzoyl chloride in toluene under gentle reflux for 1 h. Relative areas of N 1s ESCA peaks observed on these electrodes were ascertained using a Gaussian/Lorentzian peak-fitting program designed specifically for ESCA applications.[6] I_{amide}/I_{nitro} = 0.80 on a standard material, 3,5-dinitrobenzanilide, and this correction factor was applied to the electrode results. ESCA spectra were obtained using a Du Pont 650B spectrometer modified with an in-house designed microcomputer control and acquisition system.

All electrochemical experiments (cyclic voltammetry, differential pulse voltammetry, ac voltammetry) employed a conventional nonaqueous cell, with Luggin (NaSCE) reference electrode probe, and a PAR Model 174 as a potentiostat. A simple modification to this instrument allowed setting the drop life (pulse repetition rate) at 0.1–0.5 s for differential pulse voltammetry. For AC voltammetry, signals were obtained from the output of the current transducer amplifier in order to bypass output buffers and filters which are present. ac measurements utilized a PAR HR-8 lock-in amplifier for reference signal source and phase-sensitive detection. Glassy carbon electrodes were grade V10-50 from Atomergic Chemetals Corp. (Plainview, N.Y.) cut as 2.7–3 mm diameter, 4–5 mm length cylinders. All electrochemical and ESCA experiments are carried out on the cylinder ends, which are resurfaced mirror-smooth with 1-μm diamond polishing compound after each use. Solvents for electrochemistry were stored over molecular sieves (Me_2SO, CH_3CN) or distilled freshly (DMF), and uniformly contained 0.1 M $Et_4N^+ClO_4^-$ electrolyte.

Results and Discussion

Number of Amide Bonds. Previous experiments[3] showed that the binding of T(NH_2)PP to glassy carbon is associated with the presence of the amine groups on the porphyrin moiety. Formation of four amide bonds was thought unlikely on steric grounds. Analysis of the number of bonds which do form is an important part of a stereochemical picture of the modified surface.

Representing the amidization reaction as

carbon-$(COCl)_x$ + $(NH_2Ph)_4$porphyrin
→ carbon-$(CONHPh)_x$porphyrin$(PhNH_2)_{4-x}$ (2)

the residual amine sites can be determined by derivatization with a second acid chloride to form

carbon-$(CONHPh)_x$porphyrin$\left(\text{PhNHC}\langle\text{O}\rangle\text{C}_6\text{H}_3(\text{NO}_2)_2\right)_{4-x}$ (3)

The N 1s ESCA peaks of the amide and porphyrin nitrogens (400 eV) are unresolved from one another but are well resolved from nitro nitrogen (407 eV) (Figure 1). The relative areas of the two N 1s peaks provide an estimate of the percentage of free amine remaining after reaction 2. In two determinations

0002-7863/78/1500-3710$01.00/0

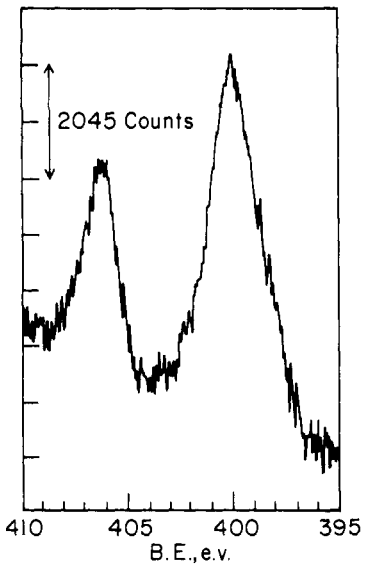

Figure 1. N 1s ESCA spectrum of glassy carbon electrode modified to bear structure shown in reaction 3.

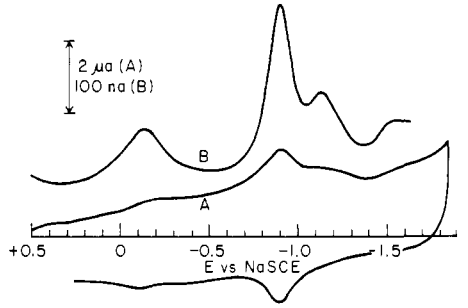

Figure 2. Cyclic voltammetry (curve A, 0.1 V/s) and differential pulse voltammetry (curve B, scan rate 2 mV/s, pulse rate 125 ms/pulse, 10 mV pulse amplitude) for a carbon-T(*p*-NH_2)PP electrode partially Co metalated, in DMF solvent with added pyridine.

using four electrode specimens each, the percentages of free amine for immobilized T(*m*-NH_2)PP were 45 ± 7 and 50 ± 13% (2σ). No correction was applied to the 400-eV peak for a small nitrogen blank present on freshly polished electrodes. Unmodified control electrodes reacted with 3,5-dinitrobenzoyl chloride exhibit no significant 407-eV (nitro) band; stable esters do not form under the conditions employed.

The free amine result indicates that $x = 2$ in reaction 2, e.g., on the average, two of the four amines of T(*m*-NH_2)PP become bound to the carbon electrode surface by an amide linkage. The distribution of mono-, bis-, and tris-bonded T(*m*-NH_2)PP which forms this average is unknown, and judging from the data scatter may vary somewhat from electrode to electrode. A predominance of bis-bonded T(NH_2)PP is, however, readily rationalized if it is assumed that the surface acid chloride site density does not greatly exceed the amine site "density" of the T(*m*-NH_2)PP. Thus the three amine groups on a freshly mono-bonded, freely rotating T(*m*-NH_2)PP have a much higher probability of encounter and reaction with an appropriately located second acid chloride site than will the two amine groups remaining on the ensuing, motionally restricted, α,β or α,γ bis-bonded species. That is, the probability of good steric register of two amine-acid chloride pairs is greater than that of three.

Further insight into the porphyrin surface bonding awaits results of experiments on the average surface acid chloride spacing and with appropriate diaminotetraphenylporphyrin isomers.

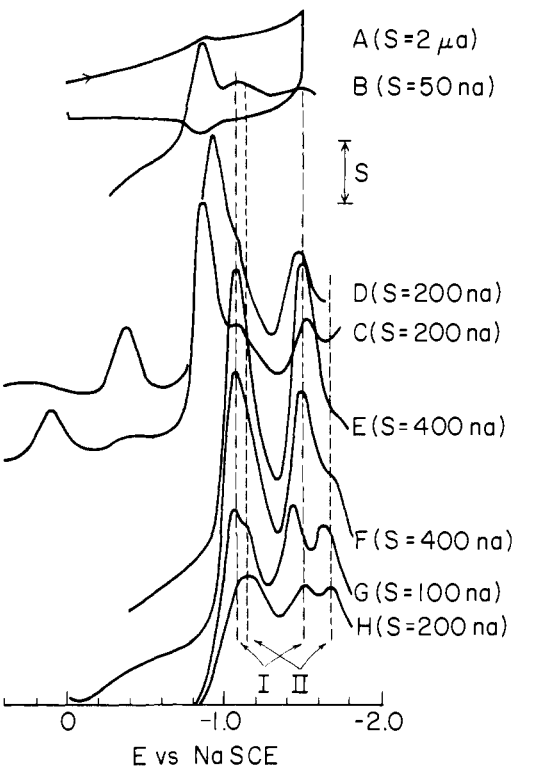

Figure 3. Cyclic voltammetry of a low coverage carbon-CoT(*m*-NH_2)PP electrode at 0.1 V/s (curve A). ac voltammetry of assorted electrodes at 10 mV/s potential sweep rate, 5 mV amplitude 40 Hz sinusoidal excitation, 90° phase detection; curve B, same electrode as curve A; curve C, mixed carbon-CoT(*m*-NH_2)PP, T(*m*-NH_2)PP electrode; curve D, same electrode as curve C with methylimidazole added to solvent; curves E and F, carbon-T(*m*-NH_2)PP electrodes; curve G, carbon-M(*p*-NH_2)TPP electrode; curve H, carbon-M(*o*-NH_2)TPP electrode. All in Me_2SO solvent. Curves offset for clarity.

Electrochemical Observation of Surface Waves. Cyclic voltammetry is readily applied to detection of chemisorbed[4,5,7,8] or synthetically linked[11-16] surface redox couples at high coverage or low background, and presently is the method of choice for systems of brief lifetime. For accurate measurements of formal potentials and ΔE_{peak} values of surface waves, especially at low sweep rates, and for characterization of surfaces at low coverages or which exhibit multiple redox processes, however, the quality of information from cyclic voltammetry can be poor (Figure 2, curve A). An alternative experiment for surface studies, differential pulse voltammetry, was introduced by Anson et al.[4,5] via a clever manipulation of uncompensated cell resistance.[9] Figure 2, curve B, illustrates the efficacy of this experiment on an electrode bearing a mixed array of T(*m*-NH_2)PP and CoT(*m*-NH_2)PP sites.

Phase selective ac voltammetry also promotes high sensitivity to surface redox events (Figure 3). Residual, unmetalated T(*m*-NH_2)PP is undetectable in the curve A cyclic voltammogram, but is discerned in the ac experiment (curve B) at a coverage estimated at 2×10^{-12} mol/cm^2. Both differential pulse and ac voltammetries detect the electrode surface capacitance dispersion which occurs at potentials for electron transfer reactions of immobilized redox couples.[10] Both methods require modest potential sweep rates (1-10 mV/s) to avoid E_{peak} shifts and demand stable (or replenished[5]) surface redox systems for prolonged observations.

C-TPP Electrodes. In Me_2SO, four reduction waves can be observed at C-T(*m*-NH_2)PP electrodes (Table I, entry 1), two (waves I) with potentials (−1.08, −1.50) closely matching those at which dissolved TPP is reduced to radical anion and dianion, and two (waves II) with low and variable amplitude

Table I. Reduction Potentials for Tetraphenylporphyrins Bound to Glassy Carbon

Entry	Solvent[a]	Electrode[b]	E_{peak}[c] vs. NaSCE Co(3/2)TPP	Co(2/1)TPP	TPP(0/−1)		TPP(−1/−2)	
1	Me_2SO	T(*m*-NH_2)PP			−1.08	(−1.14)	−1.50	(−1.70)
2	Me_2SO	M(*p*-NH_2)TPP			−1.06	−1.14	−1.45	−1.63
3	Me_2SO	M(*o*-NH_2)TPP				−1.15	−1.45	−1.63
4	Me_2SO	T(*m*-NH_2)PP + Co	+0.10	−0.86	−1.10		−1.51	
5	Me_2SO + py	T(*m*-NH_2)PP + Co	−0.18	−0.91	−1.10		−1.49	
6	Me_2SO + MeIm	T(*m*-NH_2)PP + Co	−0.39	−0.92	−1.10		−1.49	
7	CH_3CN	T(*m*-NH_2)PP				−1.32	(−1.60)	−1.83
8	CH_3CN	M(*p*-NH_2)TPP			(−1.16)	−1.31	(−1.52)	−1.76
9	CH_3CN	M(*o*-NH_2)TPP				−1.36		−1.76
10	CH_3CN	T(*p*-NH_2)PP + Co	n. obsd	−0.89		−1.37		−1.84
11	CH_3CN + MeIm	T(*p*-NH_2)PP + Co	−0.54	−1.03		−1.36	(−1.56)	−1.84
12	DMF	T(*p*-NH_2)PP + Co	+0.06	−0.83	−1.14		−1.54	
13	DMF + py	T(*p*-NH_2)PP + Co	−0.18	−0.90	−1.14		−1.54	
14	DMF + MeIm	T(*p*-NH_2)PP + Co	−0.41	−0.95	−1.14		−1.54	

[a] py = pyridine, MeIm = methylimidazole. [b] T(*m*-NH_2)PP + Co signifies an incompletely metalated electrode which exhibits electrochemistry of both T(*m*-NH_2)PP and CoT(*m*-NH_2)PP. [c] Data primarily from ac voltammetry cathodic-going scan, at potential sweep rate ≤10 mV/s. Data in parentheses represent low-intensity waves observed as shoulders or small peaks.

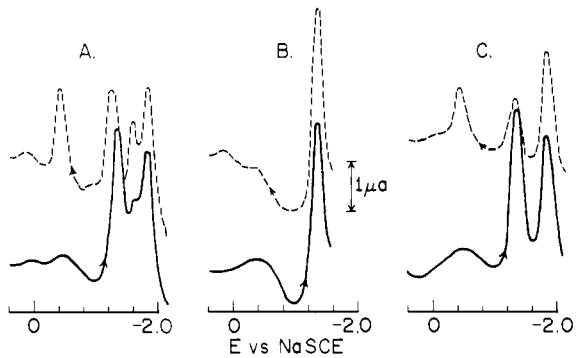

Figure 4. Cyclic ac voltammetry of carbon-T(*m*-NH_2)PP in CH_3CN solvent. 5 mV/s potential sweep rate, 5 mV amplitude, 40 Hz sinusoidal excitation, 90° phase detection. Curve A, initial cyclic scan, immediate scan reversal; curve B, pause at −1.50 V 60 s before reversal; curve C, repeat of curve A after extensive cycling.

observable only in differential pulse and ac voltammetry (Figure 3) responses.

We interpret waves I in Me_2SO and waves II in CH_3CN as

$$C\text{-}T(NH_2)PP + e \rightarrow C\text{-}T(NH_2)PP^{-}\cdot \quad (4)$$

$$C\text{-}T(NH_2)PP^{-}\cdot + e \rightarrow C\text{-}T(NH_2)PP^{2-} \quad (5)$$

The potentials for reactions 4 and 5 are shifted by −0.24 and −0.33 V in CH_3CN as compared to Me_2SO, a large solvent effect. Acetonitrile is a poor solvating medium for porphyrins, and the large shift in potential can be attributed to solvation factors, or, more plausibly, to a reactant-stabilizing interaction of the bound porphyrin system with the carbon surface which is promoted by the poor solvating efficacy of the CH_3CN medium. In view of the fact that the potential shift occurs for both T(NH_2)PP and M(NH_2)PP, and potentials for bound CoT(NH_2)PP in contrast exhibit little dependency on solvent (Table I, entries 4, 10, 12), it is further likely that the surface-porphyrin interaction involves the central ring of the bound porphyrin.

In Me_2SO solvent, reversal of the direction of potential scan yields pseudocapacitance peaks for waves I and II which are similar in amplitude and E_{peak} on cathodic and anodic-going scans. The same result is obtained in CH_3CN if scan reversal occurs (immediately or with a 60-s constant potential pause) after the radical anion-producing −1.3 V wave (Figure 4, curve B). Extension of the potential cycle to include the second, dianion wave, however, produces an attenuated *radical anion* reoxidation peak and a new wave at −0.40 (Figure 4, curve A). No effect is seen on the pseudocapacitance peak during which the dianion is oxidized, and the overall process is reversible, e.g., a subsequent cyclic ac voltammogram quantitatively repeats this pattern (curve C). Clearly production of the dianion provokes a chemical step of some kind: from its overall reversibility it is unlikely that fragmentation or protonation of the perimeter porphyrin structure has occurred. Again involvement of the central ring is most plausible. It is possible that a portion of the porphyrins are bound in such a way that the central nitrogen base sites fall in register with a surface carboxylic acid or hydroxylic site, and in CH_3CN a stabilizing, reversible proton transfer from this site to the ring nitrogen occurs (e.g., $HT(NH_2)PP^{-}$).

Interpretation of the small population of species reacting in waves II in Me_2SO and in waves I in CH_3CN is unclear. These waves decay more rapidly than the main reaction 4, 5 waves in both solvents (compare curves A, C, Figure 4). It is possible that waves II in Me_2SO represent sites for which a surface-porphyrin interaction occurs akin to that proposed to occur for the majority of bound porphyrin in CH_3CN. Experiments in which C-T(NH_2)PP electrodes are transferred between cells containing Me_2SO and CH_3CN solvent show moderately slow (~30 min) equilibration in the new solvent through slow changes in positions and relative amplitudes of waves I and II.

Mixed C-CoT(NH_2)PP, T(NH_2)PP Electrodes. Metalation reactions carried out in CH_3CN leave a residue of bound but unmetalated T(NH_2)PP whose electrochemistry serves as a convenient reference for solvent and axial ligand studies on the bound CoT(NH_2)PP. Figures 2 and 3 illustrate such mixed electrodes. Potentials of the two surface waves which appear upon cobalt metalation agree quite closely with those observed by Truxillo and Davis[17] for dissolved CoTPP complexes, and the +0.1 and −0.8 V surface waves can be identified respectively with the reactions

$$C\text{-}Co^{III}T(NH_2)PP(L)_a^{+} + e \rightarrow C\text{-}Co^{II}T(NH_2)PP(L)_b + (a-b)L \quad (6)$$

$$C\text{-}Co^{II}T(NH_2)PP(L)_b + e \rightarrow C\text{-}Co^{I}T(NH_2)PP(L)_c^{-} + (b-c)L \quad (7)$$

Potentials for reactions 4, 5 and 6, 7 are little if any affected by neighbor metalated and unmetalated sites, respectively. The potential for reaction 7 is relatively insensitive to solvent, but both it and (more strongly) reaction 6 are shifted by added

bases such as pyridine or methylimidazole (Table I, entries 4–6, 10–11, 12–14). The difference in reaction 6 and 7 potentials is 0.73 ± 0.01 V for added pyridine and 0.51 ± 0.02 V for methylimidazole, independent of solvent. The reaction 6–7 potential difference with pyridine agrees with that reported by Davis[17] for solutions of Co(TPP) containing added pyridine.

The shifts in Co porphyrin redox potentials with added ligand are clearly associated with axial coordination of the metal center, and their mere existence shows that at least one and possibly both axial sites on immobilized C-CoT(NH_2)PP are available for coordination. The magnitude of the shifts likewise suggests that ($a - b$) and ($b - c$) in reactions 6 and 7 are not altered from that in solution, although thorough potential-ligand concentration data are needed to be quantitative on this point.

Cyclic ac voltammetry is again revealing. In CH_3CN solvent with added methylimidazole (Figure 5, curve B), and in Me_2SO and DMF solvents with or without added ligand, cyclical, slow potential sweep ac voltammetry of C-CoT(NH_2)PP is approximately the same on negative and positive-going sweeps. (Some scatter using wide potential sweep ranges is attributed to hysteresis in the background signals.) In CH_3CN, in the absence of deliberately added ligand, on the other hand, the pseudocapacitance peak for the Co(I) → Co(II) reaction in the positive potential sweep is two to three times larger in amplitude, and narrower in peak width, than that for the Co(II) → Co(I) reaction (Figure 5, curve A). This effect is more pronounced at faster sweep rates (compare curves C and D). ΔE_{peak} is larger in CH_3CN than usual in Me_2SO. In conventional cyclic voltammetry on electrodes with sufficiently high coverage, a sharper (thus seemingly larger) anodic wave can be seen (curve E). The amplitude effect in the cyclic ac voltammetry primarily reflects the cathodic-anodic peak width difference; the method is more sensitive to surface wave peak width than cyclic voltammetry, as is differential pulse voltammetry.[5]

The peak width and scan rate results in CH_3CN suggest a rather slow change in cobalt axial coordination following reaction 7 in this solvent. Adventitious water, chloride, or an appropriate, underlying carbon surface functionality constitute possible ligands; whichever is involved is recoverable following reoxidation of C-Co^{I}T(NH_2)PP since the cyclic ac voltammograms are repeatable. Such analogous coordination changes as may occur in the presence of ligand or in Me_2SO solvent evidently are much more rapid, and peak width hysteresis is not seen.

The underlying basis of differing peak widths for the Co(II) → Co(I) and Co(I) → Co(II) reactions, as a consequence of the supposed coordination change, is of some interest. If interpreted in terms of nonideality interaction parameters,[5,8,18] it follows from these results that such parameters can be quite structure sensitive. An alternate explanation invokes actual structural nonuniformity (and thus a band-broadening spectrum of surface couple formal potentials $E^{0\prime}$) throughout the surface ensemble. The extent of this chemical diversity could well depend on oxidation state. If the structural readjustments following electron transfer are slow, both structural heterogeneity and nonideality parameter views anticipate a peak width difference between the cathodic and anodic reaction. As a formalism, of course, structural nonuniformity can be accommodated within the framework of nonideality parameters, as involvement of neighbor-neighbor site *interactions* is not required for nonideality. We have observed cathodic-anodic peak width differences on other occassions, for instance, the metal oxide electrode immobilized[13,19] -COPh$(NO_2)_2^{-\cdot}$ ⇄ -COPh$(NO_2)_2^{2-}$ and -tetrathiafulvaline^{+} ⇄ -tetrathiafulvaline^{2+} reactions.[20] In these cases sweep rate and structural change effects have not been identified.

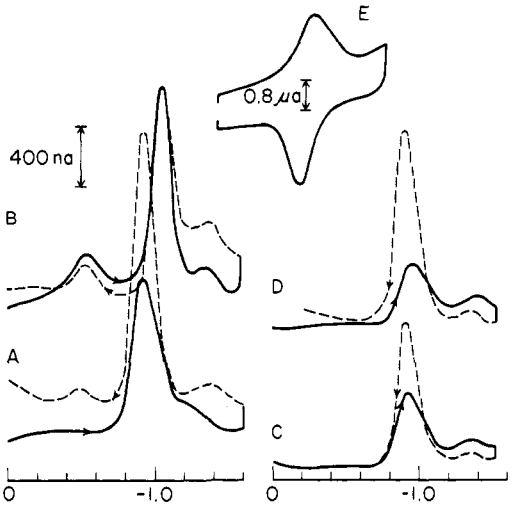

Figure 5. Cyclic ac voltammetry of mixed carbon-CoT(p-NH_2)PP, T(p-NH_2)PP electrode in CH_3CN solvent; 5 mV amplitude, 40 Hz sinusoidal excitation; 90° phase detection. Curve A, 5 mV/s potential sweep rate; curve B, 5 mV/s potential sweep rate and added methylimidazole; curve C, 2 mV/s potential sweep rate; curve D, 20 mV/s potential sweep rate; curve E, cyclic voltammetry of carbon-CoT(p-NH_2)PP electrode at 0.10 V/s, voltage axis not shown.

A comparison of the waves for reactions 6 and 7 as seen in Figures 2 and 3 (curves C, D) shows that irrespective of solvent, presence of added ligand, or method employed, the Co(III) ⇄ Co(II) porphyrin wave is broader and of substantially lower amplitude than the Co(II) ⇄ Co(I) process. The amplitude difference is doubtless in part due to the peak width sensitivity of differential pulse and ac voltammetry: interaction and/or chemical heterogeneity effects could well differ in the two reactions. In the absence of a quantitative treatment of the amplitude-peak width relation, however, we should not exclude a possible difference in charge transfer kinetics, since charge transfer rates for dissolved CoTPP complexes are fairly slow, and more so for the Co(III) ⇄ step.[17]

Finally, we previously[3] noted that electrochemical waves on C-T(NH_2)PP and C-CoT(NH_2)PP electrodes persist for many cycles. Further experience has shown that stability of the surface redox couples varies somewhat from electrode to electrode, but in general C-CoT(NH_2)PP electrochemistry is very stable, and that of C-T(NH_2)PP moderately so. Half-lives of 300–1200 s (reduced state) have been observed for C-T(NH_2)PP electrodes. One C-CoT(NH_2)PP electrode was reduced (Co(I) state) in Me_2SO for 10^4 s, then cycled 500 times in reaction 7. The reexamined reaction 7 ac voltammetric wave amplitude was (within ±10%) *unchanged* from its original value. Such stability of a ≤ monomolecular layer is remarkable. C-CoT(NH_2)PP electrodes have on several occasions been rinsed following an afternoon's experimentation, stored air dry or under solvent, and successfully reused on the next day. Potential scans into the cathodic carbon background rapidly degrade the redox ensembles.

C-T(NH_2)PP-COPh$(NO_2)_2$ Electrodes. Several specimens prepared during the amide linkage analysis of Figure 1 were examined as electrodes in DMF. Reduction waves at −0.7, −0.9, −1.2, and −1.5 V were observed using ac voltammetry; the first two waves decayed rapidly in comparison to the second two. The first and third potentials are approximately those of otherwise immobilized[12,13] -COPh$(NO_2)_2$: the other two approximate those seen on C-T(NH_2)PP electrodes. It appears that the electroactive -COPh$(NO_2)_2$ group has been immobilized on carbon electrodes using in effect the T(NH_2)PP as a bridging reagent. This is a provocative observation the possibilities of which for chemically modifying carbon are being further explored.

Discussion

These results continue to support the hypothesis that to a first approximation electrochemistry of an electrode-immobilized chemical can be anticipated from that of its dissolved counterpart. Exceptions arise, and in the present case they are provoked by use of a poorly solvating medium. It is of interest to note in this connection that solubility of a redox couple, once immobilized on the chemically modified electrode surface, is no bar to experimentation, but observed electrochemical properties may then reflect specific surface effects.

Two aspects of detailed structure of carbon-bonded tetra(aminophenyl)porphyrin were revealed in that two amide bonds form, on the average, with the carbon, and that axial sites in bonded $CoT(NH_2)PP$ are open for coordinative attack. These two features are consistent with the hypothesis that stable chemically modified surfaces are amenable to predictive electrocatalysis.[21]

Acknowledgment. This research was supported in part by the Office of Naval Research. Gift of a porphyrin sample from C. M. Elliott and support of a NSF Postdoctoral Fellowship (J.C.L.) are also acknowledged.

References and Notes

(1) To whom correspondence should be addressed.
(2) B. F. Watkins, J. R. Behling, E. Kariv, and L. L. Miller, *J. Am. Chem. Soc.*, **97**, 3549 (1975).
(3) J. C. Lennox and R. W. Murray, *J. Electroanal. Chem.*, **78**, 395 (1977).
(4) A. P. Brown, C. Koval, and F. C. Anson, *J. Electroanal. Chem.*, **72**, 379 (1976).
(5) A. P. Brown and F. C. Anson, *Anal. Chem.*, **49**, 1589 (1977).
(6) David N. Smith, University of North Carolina, unpublished results, 1976.
(7) R. F. Lane and A. T. Hubbard, *J. Phys. Chem.*, **77**, 1401, 1444 (1973).
(8) E. Laviron, *J. Electroanal. Chem.*, **47**, 2260 (1975).
(9) We have confirmed the uncompensated cell resistance dependency described by Anson,[5] and also observe additional sensitivity enhancement at shortened pulses (e.g., 0.1 s/pulse) and via the peak current–pulse amplitude (5–100 mV) proportionality.
(10) Representing the faradaic pseudocapacitance as C_f, and using a fast charge transfer equivalent circuit model,[5] the ac response to $\Delta E \sin(\omega t)$ excitation is

$$i_{ac} = \frac{\Delta E\omega(C_{dl} + C_f)}{[1 + \omega^2 R_u^2(C_{dl} + C_f)^2]^{1/2}} \sin(\omega t + \phi)$$

where $\tan\phi = [\omega R_u(C_{dl} + C_f)]^{-1}$. When $C_f \gg C_{dl}$, $\omega R_u C_f < 1$, and C_f invariant over ΔE (so $\phi = 90°$); $i_{ac} = \Delta E\omega C_f$, and $(i_{ac})_{max}$ occurs at $(C_f)_{max}$ which is at $E^{0\prime}$.
(11) P. R. Moses and R. W. Murray, *J. Am. Chem. Soc.*, **98**, 7435 (1976).
(12) P. R. Moses and R. W. Murray, *J. Electroanal. Chem.*, **77**, 393 (1977).
(13) J. R. Lenhard and R. W. Murray, *J. Electroanal. Chem.*, **78**, 195 (1977).
(14) A. Diaz, *J. Am. Chem. Soc.*, **99**, 5838 (1977).
(15) J. F. Evans and T. Kuwana, *Anal. Chem.*, **49**, 1632 (1977).
(16) M. S. Wrighton, private communication, 1977.
(17) L. A. Truxillo and D. C. Davis, *Anal. Chem.*, **37**, 2260 (1975).
(18) B. E. Conway and E. Gileadi, *Trans. Faraday Soc.*, **58**, 2493 (1962).
(19) J. R. Lenhard, unpublished results, 1977.
(20) P. R. Moses, unpublished results, 1977.
(21) J. F. Evans, T. Kuwana, M. T. Henne, and G. P. Royer, *J. Electroanal. Chem.*, **80**, 409 (1977).

Optically Active Amines. 24.[1] Circular Dichroism of the Para-Substituted Benzene Chromophore[2]

Howard E. Smith,*[3a] Elizabeth P. Burrows,[3a,4] and Fu-Ming Chen[3b]

Contribution from the Departments of Chemistry, Vanderbilt University, Nashville, Tennessee 37235, and Tennessee State University, Nashville, Tennessee 37203, and the Tennessee Neuropsychiatric Institute, Nashville, Tennessee 37217.
Received September 29, 1977

Abstract: Para substitution of chiral norephedrines causes the sign of the ^1L_b Cotton effects, negative for (αR)-norephedrine and positive for (αR)-norpseudoephedrine, to be opposite from that of the unsubstituted parent. This reversal is due to the sign change in the rotatory contribution of the chiral center adjacent to the benzene chromophore. The contribution can be subdivided into static (one-electron) as well as dynamic (coupled oscillator) mechanisms. In the unsubstituted compounds, the one-electron mechanism is dominant. On para substitution, the transition moments become larger resulting in the opposite signed contribution of the coupled oscillator mechanism overshadowing that of the one-electron mechanism. Similar considerations may also be applied to explain the sign changes on para substitution of other related chiral compounds: mandelic acid, β-hydroxy-β-phenylpropionic acid, *N*-(dichloroacetyl)norephedrine, and α-phenylethylamine. This analysis clearly indicates, however, that no single universally applicable sector rule can be devised for the prediction of the ^1L_b Cotton effects of the benzene chromophore since the one-electron and the coupled oscillator mechanisms by which the observed Cotton effects are generated make rotatory contributions of approximately equal magnitude. It appears that for open-chain chiral substituents with $\epsilon < 100$, the one-electron mechanism is dominant. With $\epsilon > 200$, the coupled oscillator mechanism may be more important.

Snatzke, Kajtar, and Warner-Zamojska[5] proposed a sector rule based on the nodal planes of the benzene ring and Platt's spectroscopic moments[6,7] by which the direction of the overall spectroscopic moment vector is used to predict the relative sign of the ^1L_b Cotton effects of chiral benzene compounds after ring substitution. In the case of a single added substituent, the rule predicts that for the ortho- and meta-substituted compounds the sign of the ^1L_b Cotton effects will be opposite to that of the parent and the para-substituted analogue if the spectroscopic moments of the original chiral group and of the added substituent are of the same sign and approximate magnitude. Experimental agreement with this prediction was noted by Snatzke[5] with the substituted phenylalanines. Both L-phenylalanine[8,9] (L-**1a**) and L-tyrosine[8,10] (L-**1b**) show a positive circular dichroism (CD) band at about 260 nm (^1L_b) while the corresponding band for L-*o*- and L-*m*-hydroxyphenylalanine (L-**1c** and L-**1d**) is negative.[10] However, observations with mandelic (**2**, R = H) and ring-substituted mandelic acids[11] (**2**) do not agree with the prediction. Snatzke[5] attributed this failure to a change in rotamer population as a result of substitution, the ring substituent affecting the hyperconjugation of the chiral group with the benzene system. More recently, similar failures of the rule have been encountered when the CD spectrum of β-hydroxy-β-phenylpropionic acid (**3**, R = H) is compared with those of its halogen-substituted derivatives (**3**).[12] The sign of the ^1L_b

0002-7863/78/1500-3714$01.00/0